BUBBLES NO MORE: TRAPPING AND REMOVAL OF GAS BUBBLES IN SINGLE-LAYER ELASTOMERIC DEVICES

C. Lochovsky[1], S. Yasotharan[1,2] and A. Günther[1,2]

[1] *Institute of Biomaterials and Biomedical Engineering, University of Toronto, CANADA*

[2] *Department of Mechanical and Industrial Engineering, University of Toronto, CANADA*

ABSTRACT

Unwanted gas bubbles are a practical problem limiting the reliable use of microfluidic systems, particularly for the culture of biological samples. We present a robust, scalable, single-layer strategy for the elimination of gas bubbles from microchannel networks that are defined in gas-permeable substrate materials. Removal rates for nitrogen bubbles were measured in water and ethanol, and compared with numerical predictions. Gas bubbles were removed at rates exceeding 0.14 µL/min in a single trap with a maximal volume of 0.43 µL. Scalability of the design was demonstrated in a parallel configuration of eight traps. The gas removal strategy was applied to the perfusion culture of small blood vessels.

KEYWORDS: Gas permeability, bubbles, bubble removal, microfluidic cell culture

INTRODUCTION

Unwanted gas bubbles in liquid-perfused microchannels present a significant practical challenge during the perfusion culture of cells, small organs or organisms. Such bubbles are often introduced through leaky world-to-chip interfaces or appear due to nucleation in heated fluid streams. The presence of bubbles can ruin experiments by blocking critical microchannel sections, or by increasing shear stresses experienced by biological samples by up to two orders of magnitude, adversely affecting biological function, and often even viability. Currently, most proposed methods are trap-only methods, or are complex solutions requiring multilayer fabrication [1-4].

EXPERIMENTAL

We propose an in-plane method for removing unwanted gas bubbles that takes advantage of the high gas permeability of poly(dimethylsiloxane) (PDMS). Bubbles enter a cylindrical trap chamber of 1 mm radius, and are prevented from passing through an array of closely spaced pillars by capillary pressure (Fig. 1a). Approximately three-quarters of the trap chamber's circumference is lined with a vacuum channel that is connected to a vacuum source. Precise fabrication using standard soft-lithography allows creation of thin membranes in the feature plane, minimizing the distance across which permeation occurs (Fig. 1b). Bubbles are removed via permeation through the interchannel wall which has an average thickness of 139 µm. The entire design has a footprint of less than 10 mm^2, allowing it to be conveniently integrated into pre-existing microchannel networks. To characterize the trap, single gas bubbles were actively formed on demand at a T-junction (Fig. 1e inset). Two miniature pneumatic valves (Lee Company, Westbrook, CT, USA) were integrated in the gas feed line off-chip, each independently actuating two normally closed on-chip valves (Fig. 1d inset) such that the bubble size could be controlled [5,6].

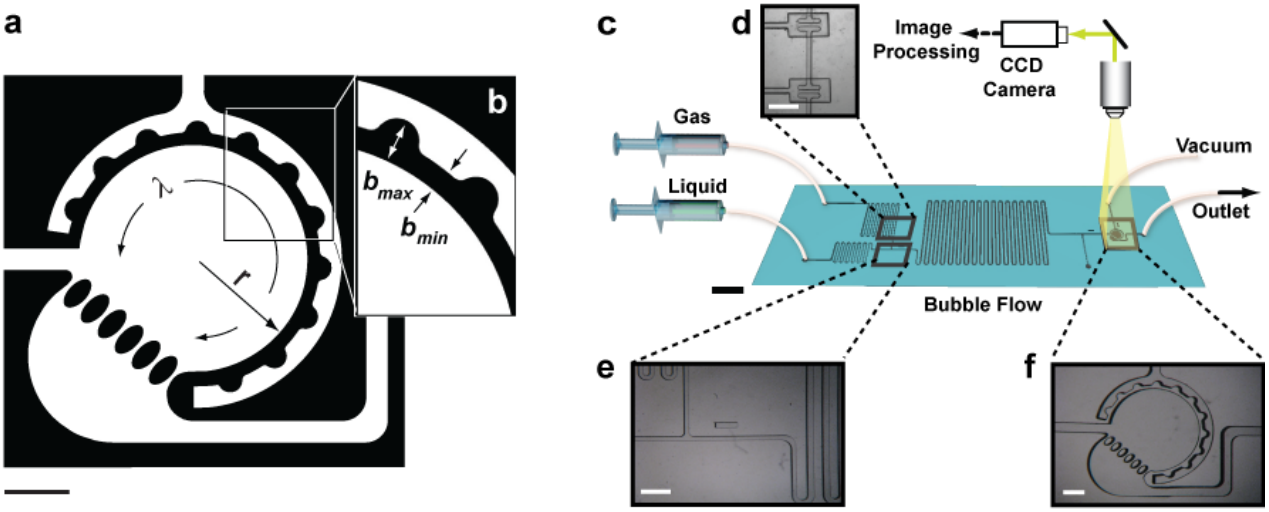

Figure 1: *Bubble trap design and experimental set-up used for characterization: (a) Microchannel networks are indicated in white, walls (PDMS) are in black. Scale bar is 500 µm. Post spacing is 50µm, radius of the trap r = 1 mm and the length of the interchannel wall, λ = 2.37 mm. For a chip with 150 µm depth, the total trap volume is 0.428 µL, and the available surface area for bubble removal is 0.71 mm^2. (b) Supports are placed every 400 µm, such that the average wall thickness is 139 µm, while the maximum thickness at the supports b_{max}=200 µm, and minimum thickness b_{min}= 100 µm elsewhere. (c) Experimental setup for measuring bubble removal rates: (d) Gas flow rate is controlled using two on-chip valves in series, which then mix with a liquid stream at a T-junction (e), creating a controlled train of bubbles which enters the trap (f), where the removal process is imaged using a CCD camera.*

RESULTS AND DISCUSSION

Bubbles were individually imaged to quantify the temporal evolution of their volumes and interfacial surface areas (Fig. 2a, 3a) from which removal rates and permeative fluxes were determined (Fig. 3b). Liquid perfusion and gas transport through the trap were numerically modeled in two dimensions using geometries obtained from these bright-field microscope images (Fig. 2b). Numerical simulations of the cross-section show that some permeative transport does occur through the top channel walls (Fig. 2c). Bubble removal rates were evaluated for the working fluids of ethanol and water and at different applied vacuum levels. For each considered bubble size and fluid, n =5 measurements were obtained. The removal rate was found to strongly depend on bubble size, and the corresponding bubble-exposed surface area of the interchannel wall. Bubbles in a solution of ethanol had lower removal rates than similarly sized bubbles in aqueous solution (Fig. 3b). The change was attributed to differences in the bubble morphology that reduced the bubble surface area in contact with the trap wall.

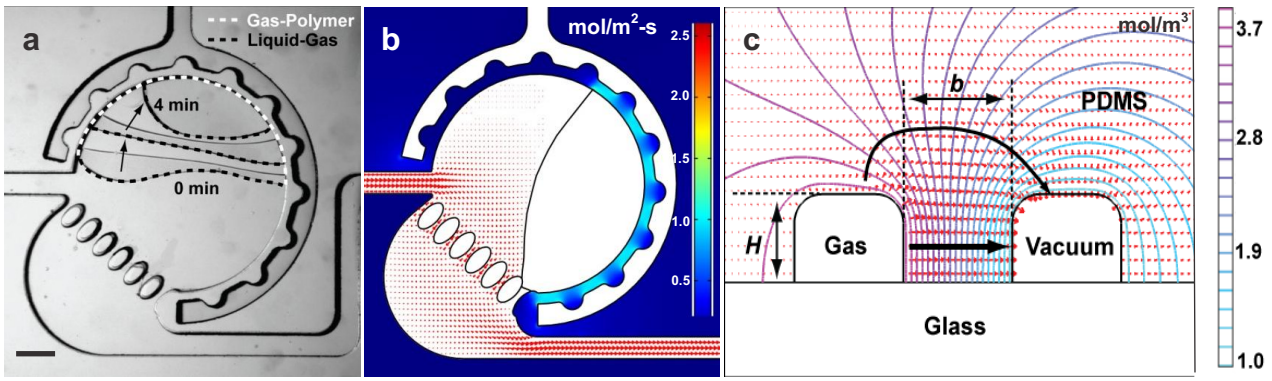

Figure 2: *(a) Contour of bubble in de-ionized water being removed with a differential pressure of 50.8kPa. The temporally evolving gas-liquid interface is highlighted by dashed black lines, the gas-solid interface by a dashed white line. Scale bar is 300 µm. (b) Experimentally obtained bubble contours were used to numerically predict the perfusion of the liquid flow through the trap as well as diffusive and convective gas transport. Colours indicate the diffusive gas flux while arrows represent the flow field of the liquid. (c) Numerical models show that while the majority of diffusive flux between gas and vacuum channels occurs between the interchannel side wall of height H=150 µm and thickness b=200 µm, some also occurs through the top walls. Arrows represent diffusive flux, while contours represent the gas concentration in the PDMS.*

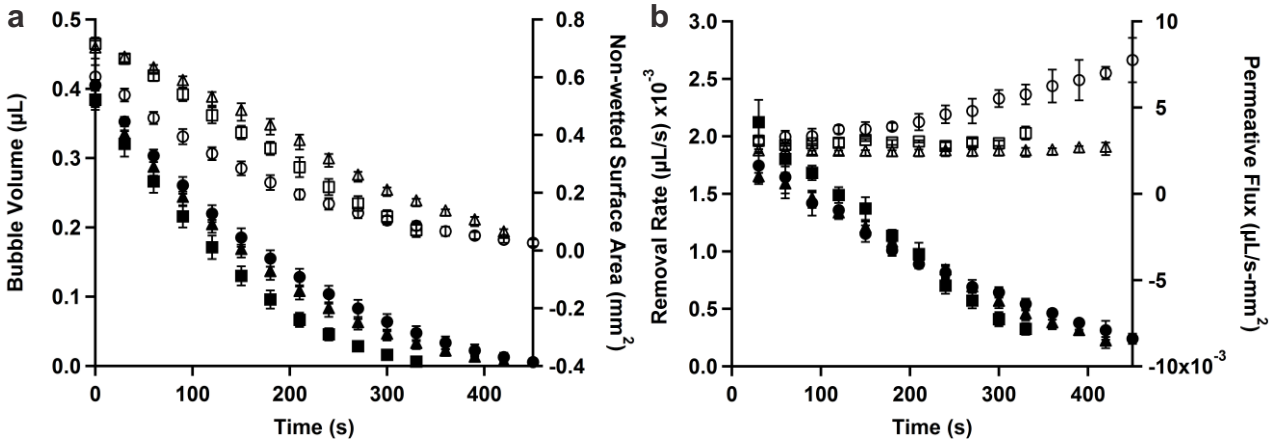

Figure 3: *(a) Comparison of evolution of bubble volume and gas-polymer surface area over time, in deionized water and ethanol, for bubbles n=5. Error bars are one standard deviation.▲ - H_2O, 74.5kPa, ■ - H_2O, 96.5kPa, ● - ethanol, 96.5kPa, solid symbols correspond to volumes, open symbols to surface areas. (b) Comparison of removal rates and permeative fluxes for the same bubbles from Fig. 3a over time, ▲ - H_2O, 74.5kPa, ■ - H_2O, 96.5kPa, ● - ethanol, 96.5kPa, solid symbols correspond to removal rate, open symbols to permeative flux. Bubbles in ethanol have significantly lower removal rates than those in deionized water.*

Preventing unwanted bubbles is crucial to small organ culture, as a single bubble damaging a region of an organ may impair overall organ function. The application of multiple traps to small organ culture was successfully demonstrated by integrating the traps with a microfluidic platform for the perfusion culture of small blood vessels (Fig. 4a) [7]. Trap scalability is an important characteristic, as increased capacity allows the removal of bubbles even from continuous segmented bubble flows generated using passive breakup. We demonstrate scalability of our strategy in an arrangement of eight parallel traps with a removal rate exceeding previously published multilayer trap designs [1]. The parallel arrangement represents the fluid mechanical analogy to solving a queuing problem, and has a total working trap volume of 4.0µL. We demonstrated removal capabilities at gas inflow rates of up to 2.0µL/min (Figs. 4b,c).

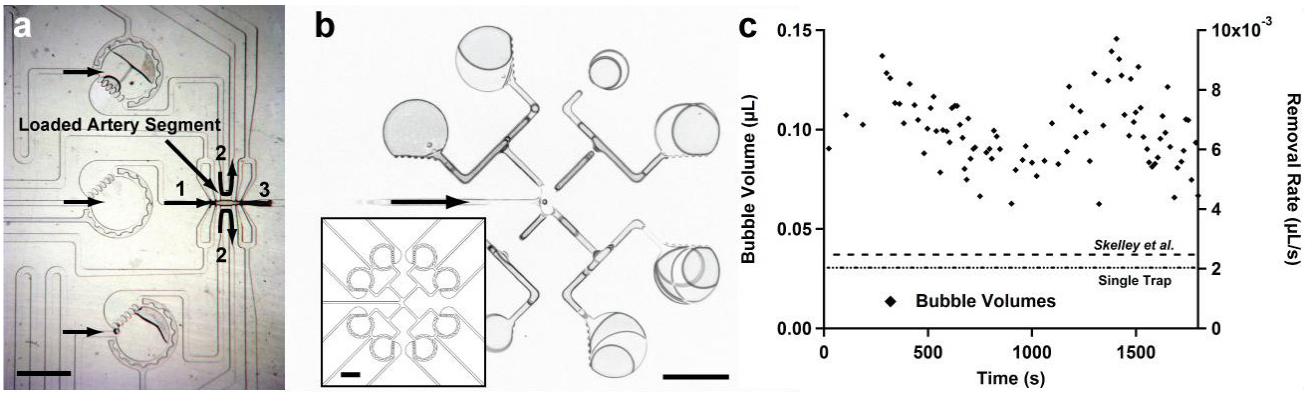

Figure 4: *Demonstrating application and scalability of the bubble trap: (a) Bubble traps applied to perfusion culture of small blood vessels. Bubble traps are indicated by arrows, in line with perfusion (labelled 1→3) and superfusion (labelled 2) flow of loaded mesenteric artery segment. (b) Time lapse overlay of bubbles in a parallel configuration of eight bubble traps where the flow direction into traps is indicated by an arrow. The corresponding microfluidic chip design is shown as an inset. Scale bars are 2mm for (a) and (b). (c) Bubble removal in the parallel trap configuration. Markers denote bubble size.*

Permeation may also be used in a reverse process to grow rather than remove bubbles. Overpressure and vacuum were used in a modified design to first shrink, and then grow gas bubbles on the same device (Fig. 5). Gas and liquid phases were mixed at a T-junction to create segmented flow. Long resistors (50cm length) were inter-digitated with gas overpressure and vacuum channels for different segments of the device. A 30kPa vacuum and 80kPa overpressure were successfully applied to shrink and grow bubbles.

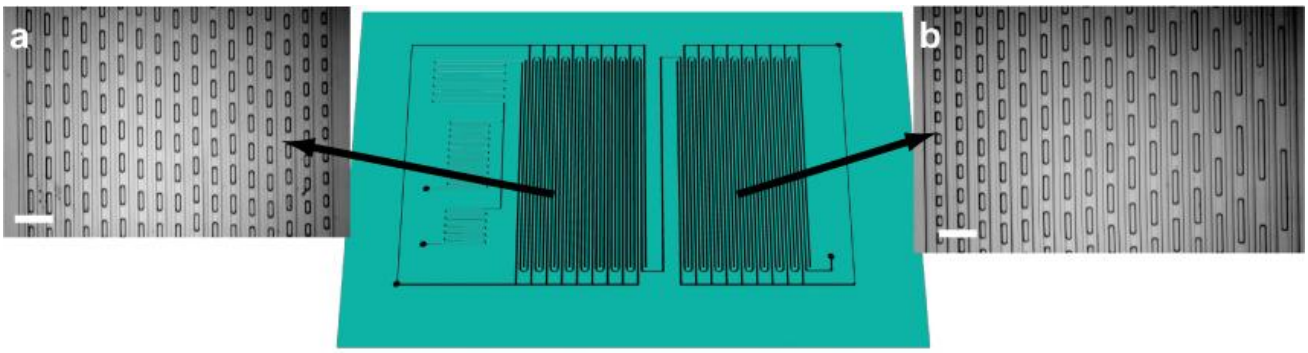

Figure 5: *Device with two sections, where bubbles in segmented flow are first shrunk using vacuum (a, inset), then grown using overpressure (b, inset). Scale bars are 1 mm.*

ACKNOWLEDGEMENTS

We thank Faisal Moledina, John Nguyen, Sascha Pinto, and Till Richter for their contributions, and acknowledge funding from the Natural Sciences and Engineering Research Council of Canada (Idea to Innovation Award, AG), the Canada Foundation for Innovation (AG), the Ontario Ministry for Research and Innovation (AG), an Ontario Graduate Scholarship (CL) and a Barbara and Frank Milligan Fellowship (CL).

REFERENCES

[1] J. Kang, Y. Kim, and J. Park, "Analysis of pressure-driven air bubble elimination in a microfluidic device," Lab on a Chip, **8**, 176 (2008).

[2] A. Skelley and J. Voldman, "An active bubble trap and debubbler for microfluidic systems," Lab on a Chip, **8**, 1733 (2008).

[3] J. Sung and M. Shuler, "Prevention of air bubble formation in a microfluidic perfusion cell culture system using a microscale bubble trap," Biomedical Microdevices, **11**, 731 (2009).

[4] Z. Yang, S. Matsumoto, and R. Maeda, "A prototype ultrasonic micro-degassing device for portable dialysis system," Sensors and Actuators A, **95**, 274 (2002).

[5] D. Irimia and M. Toner, "Cell handling using microstructured membranes," Lab on a Chip, **6**, 345 (2006).

[6] S. Zeng, B. Li, X. Su, J. Qin, and B. Lin, "Microvalve-actuated precise control of individual droplets in microfluidic devices," Lab on a Chip, **9**, 1340.

[7] A. Günther, S. Yasotharan, A. Vagaon, C. Lochovsky, S. Pinto, J. Yang, C. Lau, J. Voigtlaender-Bolz, and S.S. Bolz, "A microfluidic platform for probing small artery structure and function," Lab on a Chip, in press.